

Investigation of a New Hybrid Excitation Machine with Auxiliary Winding for Energy Recycling

Xing Zhao, Shuangxia Niu

Department of Electrical Engineering, Hong Kong Polytechnic University, Hong Kong

Abstract- From a new stator-flux perspective, a comparative study between the series and parallel hybrid excitation machine (PHEM) is conducted and it is revealed that in PHEMs there still exists distinct stator flux harmonic components during high-speed flux weakening operation, which could be further utilized to improve the torque capability at high-speed range. Inspired by this idea, an auxiliary winding is creatively introduced into PHEMs to recycle and utilize the magnetic field energy generated during the field regulation. A new design case is presented in this paper, in which two sets of armature windings with different pole pair numbers are arranged to realize the function of flux weakening operation and energy recycling, respectively. The feasibility of this new hybrid solution is evaluated by using the finite element analysis. Furthermore, a prototype is manufactured and relevant experiments are performed. The experimental results agree well with the theoretical analysis and simulation results, which verify that the recycled energy can be effectively used to boost the output torque and power of PHEMs in the high-speed region.

Index Terms—Parallel hybrid excitation, stator flux, auxiliary winding, energy recycling.

I. INTRODUCTION

Permanent magnet (PM) machine has been widely studied due to its high torque density and high efficiency. Nevertheless, in some variable speed applications such as electric vehicles and household appliances, good flux weakening capability and corresponding wide constant power range are also required.

Hybrid excitation machine (HEM), which employs both PM excitation and field excitation, has attracted much attention in literature for its excellent flux weakening ability [1]. There is a variety of HEM topologies to be investigated. In general, from the perspective of magnetic circuit, HEMs can be divided into two typical groups, series hybrid excitation machines (SHEM) [2] and parallel hybrid excitation machines (PHEM) [3-4]. Compared with the parallel structure, SHEM has a simpler structure. However, there are some disadvantages for SHEMs. Due to the low permeability of the PMs, the reluctance for the field path is quite high. Therefore, a large ampere-turn field MMF is needed to weaken PM magnetic field. Furthermore, demagnetization risk inevitably exists in series topologies. As for the PHEMs, the PMs are not in the magnetic circuit of the field winding, thus providing an improved field-regulating capability and zero demagnetization risk.

However, HEMs suffer from the reduced torque density and considerable copper loss during the flux weakening operation. Specially, when the HEM exceeds the base speed, copper loss generated by the field excitation continuously increases since the higher speed needed, the larger field excitation should be applied to weaken the PM field. Meanwhile, the torque density decreases due to the weakened flux density. However, authors find in some HEMs, especially some parallel structures, the field excitation not only works to weaken the PM magnetic field, but also generate new stator flux. Inspired by that, a new design method is proposed in this paper, aimed at recycling the magnetic field energy of HEMs during field regulation and further improving its performance in the high-speed region.

In the following paper, difference in the flux weakening phenomenon between the SHEMs and PHEMs will be studied from a new stator flux perspective, and based on that, a novel design method is proposed for PHEMs, in which an auxiliary winding is introduced for the energy recycling. Then, a new design case will be presented and a prototype is manufactured for the experimental verification.

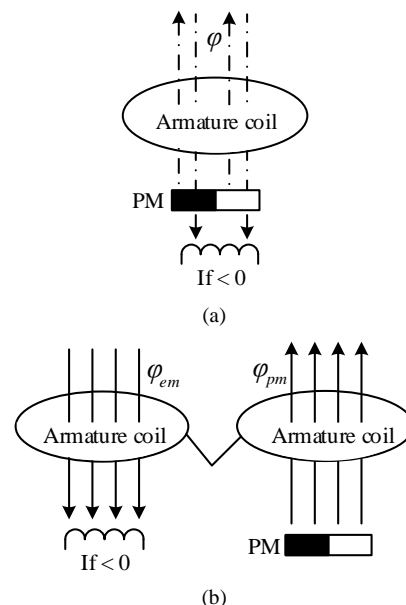


Fig. 1. Schematic views of flux weakening. (a) In SHEM. (b) In PHEM.

II. COMPARATIVE STUDY AND A NEW DESIGN APPROACH

A. Difference in flux weakening from a stator flux perspective.

Fig. 1 shows schematic views of flux weakening operation in SHEMs and PHEMs, respectively. One can see, in SHEMs, the field MMF and PM MMF have the same magnetic flux paths as shown in Fig. 1(a). Therefore, when the field MMF is increased to a certain level and the synthetic MMF is close to zero, flux linkage in the stator armature coil will decrease to zero synchronously. Different from that, in PHEMs, these two excitation sources usually have independent magnetic flux

paths as described in Fig. 1(b). And when the flux weakening operation occurs, flux linkage in the separated armature coils generated by the field and PM MMF, respectively, will have similar values and the cascaded flux will approach zero.

From a stator flux perspective, a significant difference can be found between SHEMs and PHEMs during flux weakening, that is, stator flux in the armature coil of SHEM will decrease to zero, while in PHEMs, distinct stator flux still exists in the separated armature coils.

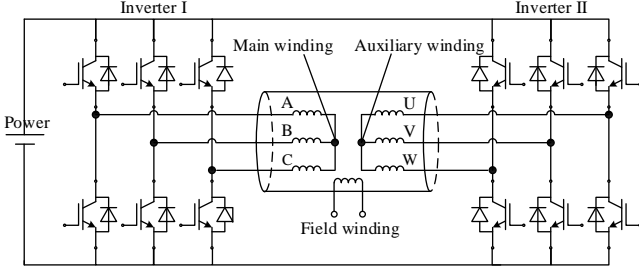


Fig. 2. Proposed drive system.

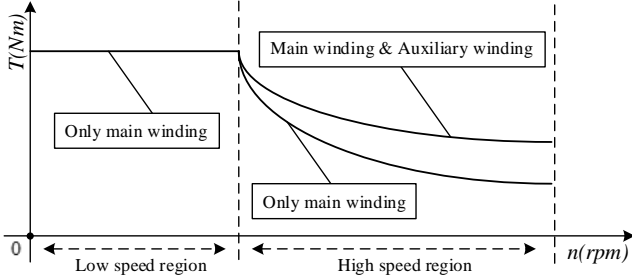


Fig. 3. Operation mode in a whole speed region.

B. New approach to utilize the stator flux in PHEMs

Based on the above analysis, there is still distinct stator flux in PHEMs during flux weakening operation. Furthermore, this stator flux is no longer synchronized with original armature winding. Inspired by this phenomenon, a new design method is proposed in this paper, aiming to further utilize this stator flux so as to improve the electromagnetic performance in PHEMs. More specifically, an auxiliary winding is artificially introduced into PHEMs to interact with the asynchronous stator field during flux weakening operation. Correspondingly, induced voltage can be obtained in the auxiliary winding. By further injecting alternating armature current into this auxiliary winding, extra electromagnetic torque can be achieved.

The whole machine system is described in Fig. 2. One can see, there are three set of windings arranged in the PHEM, namely the main winding, auxiliary winding and field winding, respectively. The main winding and field winding play the same roles as those in the conventional PHEMs, while the auxiliary winding takes charge of interacting with provoked magnetic field during flux weakening operation. Two inverters are adopted to regulate the armature current for main winding and auxiliary winding, respectively, and they share a common power source and DC bus. The operation mode is illustrated in Fig. 3. In low speed region, only the main winding makes contribution to the torque generation. When a field current is applied for flux weakening, the auxiliary winding starts to effectively interact with the stator flux, so it can work at the

same time with the main winding. Therefore, the output torque and power density can be enhanced in the high-speed region.

III. A NEW DESIGN CASE

To verify the feasibility of this new hybrid solution, a new design case is presented which integrates an auxiliary winding for the energy recycling during flux weakening operation. The machine configuration, operation principle and corresponding winding design criterions will be discussed.

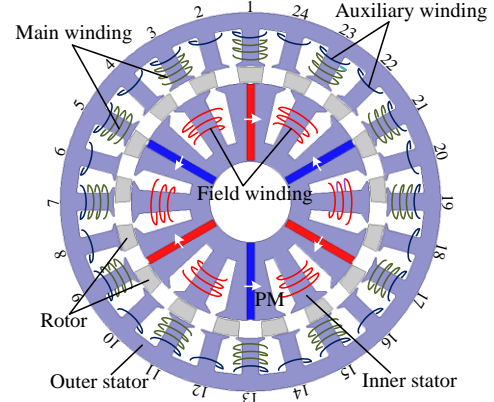


Fig. 4. Configuration of the proposed PHEM.

A. Machine configuration

The proposed PHEM configuration is presented in Fig. 4, which comprises two separate stators and a sandwiched sliced rotor. One can see, there are two sets of armature windings arranged in the outer stator, namely the main winding and auxiliary winding, respectively. The sliced rotor is composed of evenly distributed magnetic steel segments. The inner stator acts as a hybrid excitation source which mainly consists of steel laminations, tangentially magnetized PMs as well as non-overlapping concentrated field coils. Adjacent field coils have opposite polarities and they are connected in series to form a single field winding. It should be mentioned the configuration of inner stator in the proposed PHEM, is similar to the rotor of the existed HEM in [5], however, the field winding is moved to the static body, and thus slip ring and brush are eliminated. Meanwhile, this double-stator structure can enhance the space utilization ratio since all the field winding, PMs and armature windings have no space conflict with each other.

Due to the sliced-type rotor, flux modulation effect exists in the proposed machine [6]. The magnetic field produced by the inner excitation source is no longer uniform, instead, a large number of harmonic components will be produced and their pole pair number (PPN) can be obtained from

$$PPN_{m,k} = |mp_s + kp_r| \quad (1)$$

$$m = 1, 3, 5, \dots, k = 0, 1, 2, 3, \dots$$

where p_s is the PPN of the inner excitation source, p_r is the number of modulation steel segments.

The corresponding rotational velocities of each harmonic component are

$$\omega_{m,k} = \frac{kp_r}{mp_s + kp_r} \omega_r \quad (2)$$

where ω_r is the rotational velocity of modulation rotor.

With this flux modulation effect, harmonics with the same pole pair number and same rotational speed as those of the armature field will interact with each other. To get the highest transmitted electromagnetic torque, the number of modulation steel segments, PPN of inner excitation sources, and PPN of the armature windings, are governed by

$$p_r = p_s + p_a \quad (3)$$

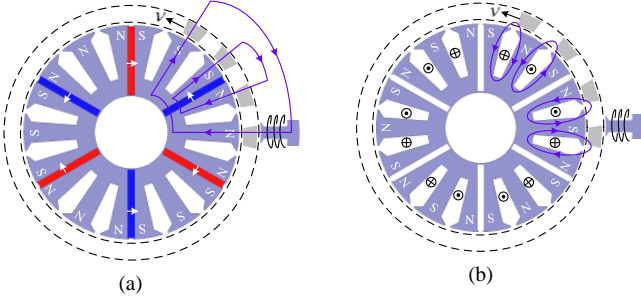


Fig. 5. Schematic flux distribution. (a) Only PMs. (b) Only field excitation.

B. Operation principle of flux weakening

Fig. 5 presents its operation principle of flux weakening. When only the PM excitation is active, the flux distribution is shown in Fig. 5(a). It can be seen the effective flux starts from the inner PMs, then passing through the modulation rotor to interact with armature windings in the outer stator, and finally comes back to the PMs again. Fig. 5(b) presents the flux distribution when there is only field excitation. The effective flux starts from the inner wound poles, then is shorted by the modulation rotor and comes back through the adjacent iron cores. It is obvious this field flux doesn't pass through the PMs, thus belonging to a parallel magnetic circuit.

Furthermore, one can see the PPN of the field excitation (9-pole-pair, denoted in the form of NSNSNS), is different from that of the PM excitation (3-pole-pair, denoted in the form of NNNSSS). Which means, when a field current is applied, PPN of the hybrid excitation source can be changed, and hence, a pole-changing flux weakening operation can be realized [7].

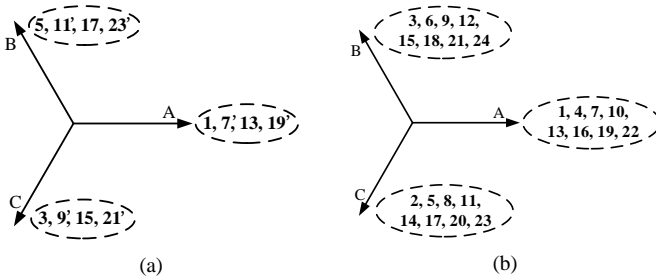


Fig. 6. Winding connections. (a) Main winding. (b) Auxiliary winding.

C. Winding Design

Considering it is the first time in literature to introduce an auxiliary winding into PHEMs, its design criterion should be clearly illustrated. Generally speaking, the design criterion for the armature windings should be governed by the Equ. (3). It can be seen the winding PPN is determined by the number of modulation steel segments as well as the PPN of the inner excitation source. The number of steel segments is a constant once the design parameter is determined, however, the PPN of

the inner excitation source is not fixed, which actually can be changed by applying different field current as analyzed above. Therefore, the key to design two sets of armature windings, is dependent on the PPN of inner excitation source that they actually interact with. The main winding aims at interacting with PM excitation in the whole speed range, so it should be designed according to the PPN of PM excitation without any field current. As for the auxiliary winding, it is introduced to interact with the hybrid excitation source when field current is applied. Therefore, it should be designed according to the PPN of the hybrid excitation source with rated field current.

In the proposed PHEM case, the number of steel segments is selected as 17 and the PPN of PM excitation is 3. Therefore, from Equ.(3), the PPN of the main winding should be set at 14. Similarly, the PPN of hybrid excitation with rated field current is 9, and accordingly, the PPN of the auxiliary winding should be 8. There are 24 slots arranged in the outer stator and Fig. 6 gives the winding connections with corresponding slot pole combinations. Specifically, the main winding adopts a single-layer reverse connection, while the auxiliary winding adopts a double-layer forward connection.

TABLE I
Design parameters of the proposed machine

Parameter	Unit	Value
Outer dimension of the outer stator	mm	150
Inner dimension of the outer stator	mm	108
Outer dimension of the inner stator	mm	94
Inner dimension of the inner stator	mm	32
Axial length	mm	80
Outer air gap length	mm	0.5
Inner air gap length	mm	0.5
Turn number of each main coil	-	38
Turn number of each auxiliary coil	-	8

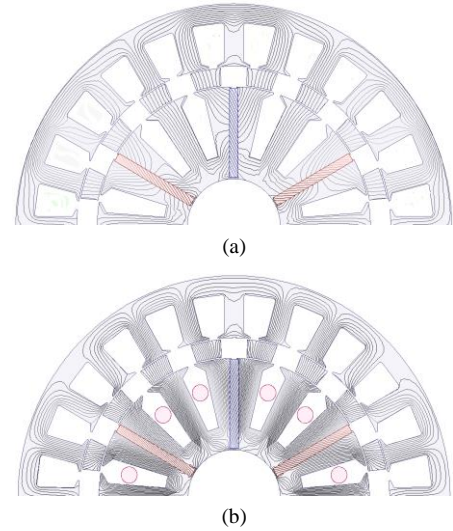


Fig. 7. Magnetic field distribution. (a) Full level with only PM excitation. (b) Weak level with 9.5A field excitation.

I. FINITE ELEMENT ANALYSIS

A. Magnetic field distribution

To verify the feasibility of this new hybrid solution, a finite element model is established with relevant design parameters listed in the Table I. Fig. 7 shows the no load magnetic field

distribution at two typical excitation states. One can see, there is still distinct stator flux during the flux weakening operation compared with that when only the PM excitation is active, and its distribution shape has changed. This phenomenon is mainly caused by the parallel feature and agrees with the special flux weakening phenomenon in PHEMs as previously discussed.

The flux density in the outer air gap is plotted in Fig. 8(a). Further, by using Fourier analysis, its harmonic distribution is calculated and presented in Fig. 8(b). It can be seen, when there is only PM excitation, the main harmonics are the 3th, 14th and 20th one, respectively. These main harmonics can synchronously interact with the 14-PPN main winding, and meanwhile, less flux will be generated in the asynchronous auxiliary winding. When the flux weakening operation occurs, these original main harmonics all present a decrease, while the 8th and 9th one increase to a distinct level, which can interact with the 8-PPN auxiliary winding effectively. The results of harmonic analysis agree well with the previous considerations during the winding design process.

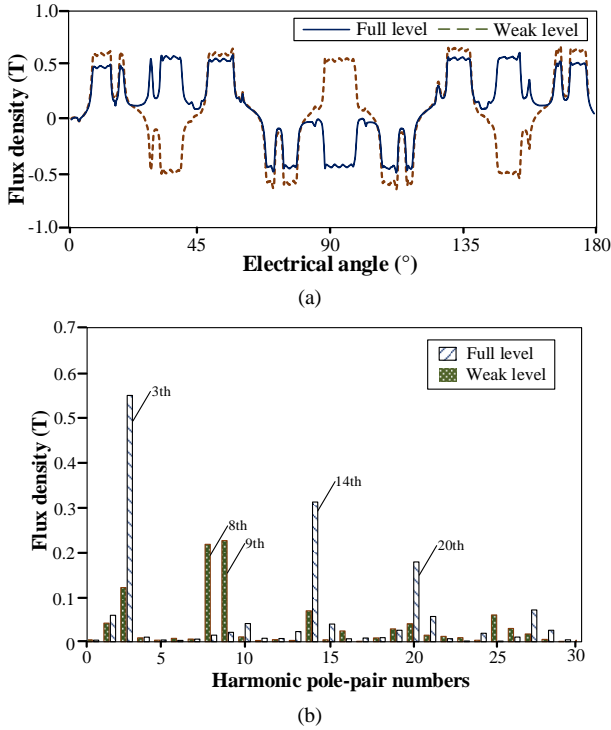


Fig. 8. (a) Outer air gap flux density. (b) Harmonics analysis.

B. Back EMF

Fig. 9 shows the back EMF of two set of armature windings with different field excitation. It can be seen, with the increase of field current, the back EMF amplitude of the main winding decreases from 46V to 18V, which proves the flux weakening ability of the proposed PHEM. And meanwhile, the back EMF amplitude of the auxiliary winding presents an opposite trend and increases from 8V to 29V, thus verifying its capability to recycle the magnetic field energy during field regulation.

A. Electromagnetic torque

By injecting sinusoidal current into this auxiliary winding, extra electromagnetic torque can be acquired. Fig. 10 shows the calculated steady torque waveforms at weak level. It can

be seen, with the same armature current injected, the auxiliary winding can acquire a comparable torque with that of the main winding, therefore, when these two sets of windings work at the same time, two torque components generated by the main winding and auxiliary winding, respectively, will overlap in the rotor and thus the synthetic output torque can be enhanced.

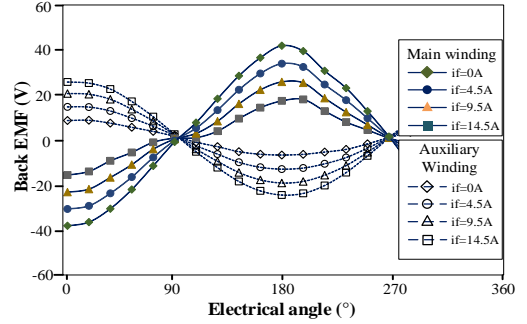


Fig. 9. Back EMF with different field excitation.

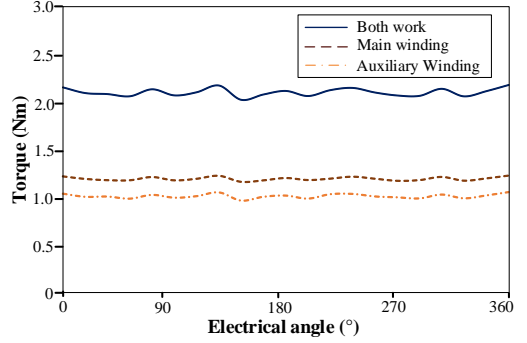


Fig. 10. Steady torque at weak level with 5A armature current.

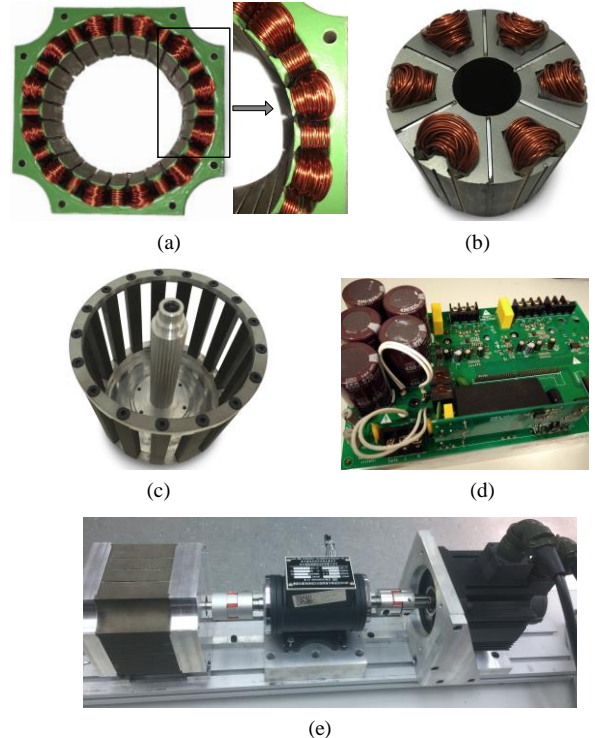


Fig. 11. Prototype, drive circuit and test bed. (a) Outer stator. (b) Inner stator. (c) Sliced rotor. (d) Integrated two inverters. (e) Test bed.

II. EXPERIMENTAL VERIFICATION

The machine prototype is manufactured with relevant key components presented in Fig. 11, including the outer stator, inner stator and rotor, respectively. The outer stator consists of the steel laminations and two sets of armature windings as highlighted. The inner stator is composed of steel laminations, tangentially magnetized PMs and concentrated field coils. Considering mechanical strength requirement, the sliced rotor is not laminated, and instead, discrete steel bars are fixed by two end plates and lock screw to form a complete rotor. A test bed is also built based on the prototype

The induced voltage of two sets of armature windings are measured in Fig. 12. It can be seen, when the field current is not applied, the back EMF in the main winding is much larger than that in the auxiliary winding. Furthermore, the back EMF curves against field current is presented in Fig. 13. With the field current increasing, the back EMF in the main winding decreases as expected, while that in the auxiliary winding shows an opposite variation trend. An acceptable difference exists between measured values and FEA predictions, which is mainly caused by the prototype fabrication tolerance.

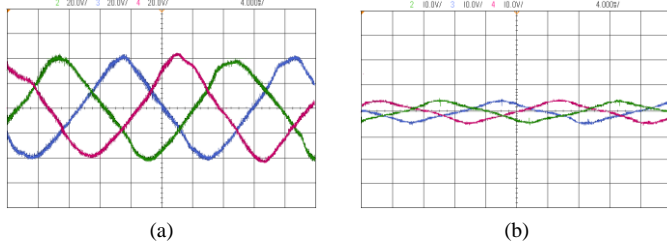


Fig. 12. Measured back EMF without field excitation, at 600rpm. (a) Main winding. (b) Auxiliary winding.

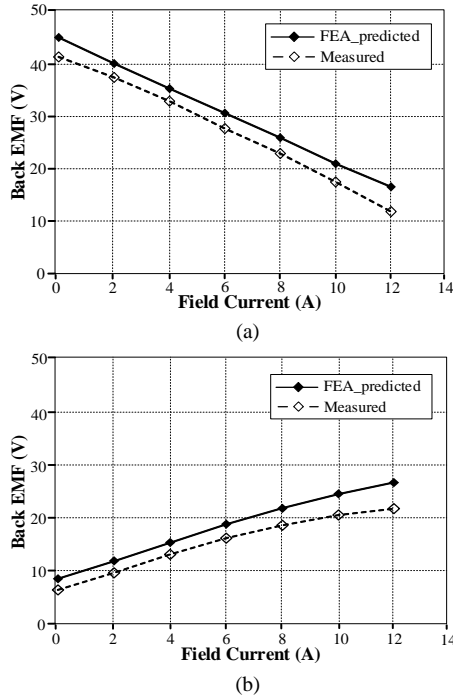


Fig. 13. Measured back EMF curve against field excitation, at 600rpm. (a) Main winding. (b) Auxiliary winding.

Further, the torque-speed curve is measured and plotted in Fig. 14, with the limit of 100 V dc bus voltage. The base speed of the proposed machine is set at 600 rpm. One can see, by

applying the field excitation, flux weakening operation can be achieved which leads to an extended speed range. Besides, due to the introduction of auxiliary winding, the output torque can be significantly boosted in high speed region, which verifies the effectiveness of this new hybrid solution.

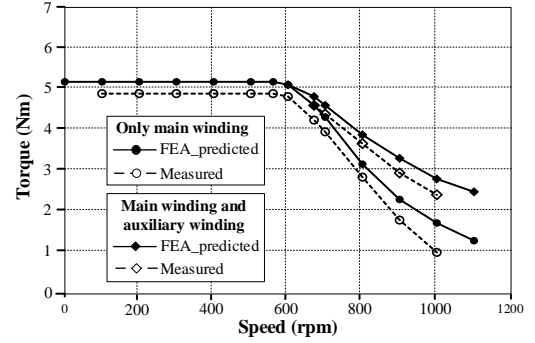


Fig. 14. Measured torque-speed curves.

III. CONCLUSION

In this paper, difference in flux weakening between SHEMs and PHEMs, is investigated from a new stator flux perspective. It is found in PHEMs, the flux weakening effect is essentially realized by making stator flux asynchronous with the armature windings. Inspired by that, an auxiliary winding is creatively introduced into PHEMs to interact with the asynchronous magnetic field generated during field regulation. After that, a design case is presented which integrates an auxiliary winding for energy recycling. The feasibility of this solution is further verified by both finite element analysis and prototype testing. Relevant results reveal that the recycled energy can be utilized to boost the torque density and output power in the high-speed region. It should be pointed out this new design method is not only restricted to the design case in this paper, which may be also applied to other PHEMs.

IV. ACKNOWLEDGEMENT

This work was supported by the Research Project PolyU 152193/15E, and project 4-ZZBM of Hong Kong Polytechnic University, Hong Kong.

V. REFERENCES

- [1] J. A. Tapia, F. Leonardi, and T. A. Lipo, "Consequent-pole permanent magnet machine with extended field-weakening capability," *IEEE Trans. Ind. Appl.*, vol. 39, no. 6, pp. 1704–1709, Dec. 2003.
- [2] H. Hua, Z. Q. Zhu, and H.L. Zhan, "Novel Consequent-Pole Hybrid Excited Machine With Separated Excitation Stator," *IEEE Trans. Ind. Electron.*, vol. 63, no. 8, pp. 4718–4728, Aug. 2016.
- [3] L. Xu, Wenxiang Zhao, Jinghua Ji, et al., "Design and Analysis of a New Linear Hybrid Excited Flux Reversal Motor with Inset Permanent Magnets," *IEEE Trans. Magn.*, vol. 50, no. 11, pp. 1–4, Nov. 2014.
- [4] W. Geng, Z. Zhang, K. Jiang and Y. Yan, "A New Parallel Hybrid Excitation Machine: Permanent-Magnet/Variable-Reluctance Machine with Bidirectional Field-Regulating Capability," *IEEE Trans. Ind. Electron.*, vol. 62, no. 3, pp. 1372–1381, Mar. 2015.
- [5] Y. Amara, L. Vido and M. Gabsi, "Hybrid excitation synchronous machines: Energy-efficient solution for vehicles propulsion," *IEEE Trans. Veh. Technol.*, vol. 58, no. 5, pp. 2137–2149, Jun. 2009.
- [6] Z. Wu; Z. Zhu, "Analysis of Magnetic Gearing Effect in Partitioned Stator Switched Flux PM Machines," *IEEE Trans. Energy Convers.*, vol. 99, no. 1, pp. 1–1, Oct. 2016.
- [7] F. Li, K. T. Chau and C. Liu, "Pole-Changing Flux-Weakening DC-Excited Dual-Memory Machines for Electric Vehicles," *IEEE Trans. Energy Convers.*, vol. 31, no. 1, pp. 27–36, March 2016.